

# New Diphosphine Ligands Containing Ethyleneglycol and Amino Alcohol Spacers for the Rhodium-Catalyzed Carbonylation of Methanol

Christophe M. Thomas, Roger Mafua, Bruno Therrien<sup>+</sup>, Eduard Rusanov<sup>+</sup>, Helen Stöckli-Evans<sup>+</sup>, and Georg Süß-Fink<sup>\*[a]</sup>

**Abstract:** The new diphosphine ligands  $\text{Ph}_2\text{PC}_6\text{H}_4\text{C}(\text{O})\text{X}(\text{CH}_2)_2\text{OC}(\text{O})\text{C}_6\text{H}_4\text{PPh}_2$  (**1**: X = NH; **2**: X = NPh; **3**: X = O) and  $\text{Ph}_2\text{PC}_6\text{H}_4\text{C}(\text{O})\text{O}(\text{CH}_2)_2\text{O}(\text{CH}_2)_2\text{OC}(\text{O})\text{C}_6\text{H}_4\text{PPh}_2$  (**5**) as well as the monophosphine ligand  $\text{Ph}_2\text{PC}_6\text{H}_4\text{C}(\text{O})\text{X}(\text{CH}_2)_2\text{OH}$  (**4**) have been prepared from 2-diphenylphosphinobenzoic acid and the corresponding amino alcohols or diols. Coordination of the diphosphine ligands to rhodium, iridium, and platinum resulted in the formation of the square-planar complexes  $[(\text{P}-\text{P})\text{Rh}(\text{CO})\text{Cl}]$  (**6**: P–P = **1**; **7**: P–P = **2**; **8**: P–P = **3**),  $[(\text{P}-\text{P})\text{Rh}(\text{CO})\text{Cl}]_2$  (**9**: P–P = **5**),  $[(\text{P}-\text{P})\text{Ir}(\text{cod})\text{Cl}]$  (**10**: P–P = **1**; **11**: P–P = **2**; **12**: P–P = **3**),  $[(\text{P}-\text{P})\text{Ir}(\text{CO})\text{Cl}]$  (**13**: P–P = **1**; **14**: P–P = **2**; **15**: P–P = **3**), and  $[(\text{P}-\text{P})\text{PtI}_2]$  (**18**: P–P = **2**). In all complexes, the diphosphine ligands are *trans* coordinated to the metal center, thanks

to the large spacer groups, which allow the two phosphorus atoms to occupy opposite positions in the square-planar coordination geometry. The *trans* coordination is demonstrated unambiguously by the single-crystal X-ray structure analysis of complex **18**. In the case of the diphosphine ligand **5**, the spacer group is so large that dinuclear complexes with ligand **5** in bridging positions are formed, maintaining the *trans* coordination of the P atoms on each metal center, as shown by the crystal structure analysis of **9**. The monophosphine ligand **4** reacts with  $[\text{Ir}(\text{cod})\text{Cl}]_2$  (cod = cyclooctadiene) to give the simple derivative  $[(\text{4})\text{Ir}(\text{cod})\text{Cl}]$

(**16**) which is converted into the carbonyl complex  $[(\text{4})\text{Ir}(\text{CO})_2\text{Cl}]$  (**17**) with carbon monoxide. The crystal structure analysis of **16** also reveals a square-planar coordination geometry in which the phosphine ligand occupies a position *cis* with respect to the chloro ligand. The diphosphine ligands **1**, **2**, **3**, and **5** have been tested as cocatalysts in combination with the catalyst precursors  $[\text{Rh}(\text{CO})_2\text{Cl}]_2$  and  $[\text{Ir}(\text{cod})\text{Cl}]_2$  or  $[\text{H}_2\text{IrCl}_6]$  for the carbonylation of methanol at 170 °C and 22 bar CO. The best results (TON 800 after 15 min) are obtained for the combination **2**/  $[\text{Rh}(\text{CO})_2\text{Cl}]_2$ . After the catalytic reaction, complex **7** is identified in the reaction mixture and can be isolated; it is active for further runs without loss of catalytic activity.

**Keywords:** amino alcohols • homogeneous catalysis • phosphane ligands • rhodium

## Introduction

The carbonylation of methanol to give acetic acid is one of the most important homogeneously catalyzed industrial processes.<sup>[1]</sup> The catalytic reaction requires the use of iodide promoters which convert methanol, prior to carbonylation, into the actual substrate methyl iodide.<sup>[2]</sup> The original  $[\text{Rh}(\text{CO})_2\text{I}_2]^-$  catalyst, developed at the Monsanto laboratories<sup>[3, 4]</sup> and studied in detail by Forster and co-workers,<sup>[5–7]</sup> is largely used for the industrial production of acetic acid and acetic anhydride. The rate-determining step of the catalytic cycle is the oxidative addition of  $\text{CH}_3\text{I}$  to give

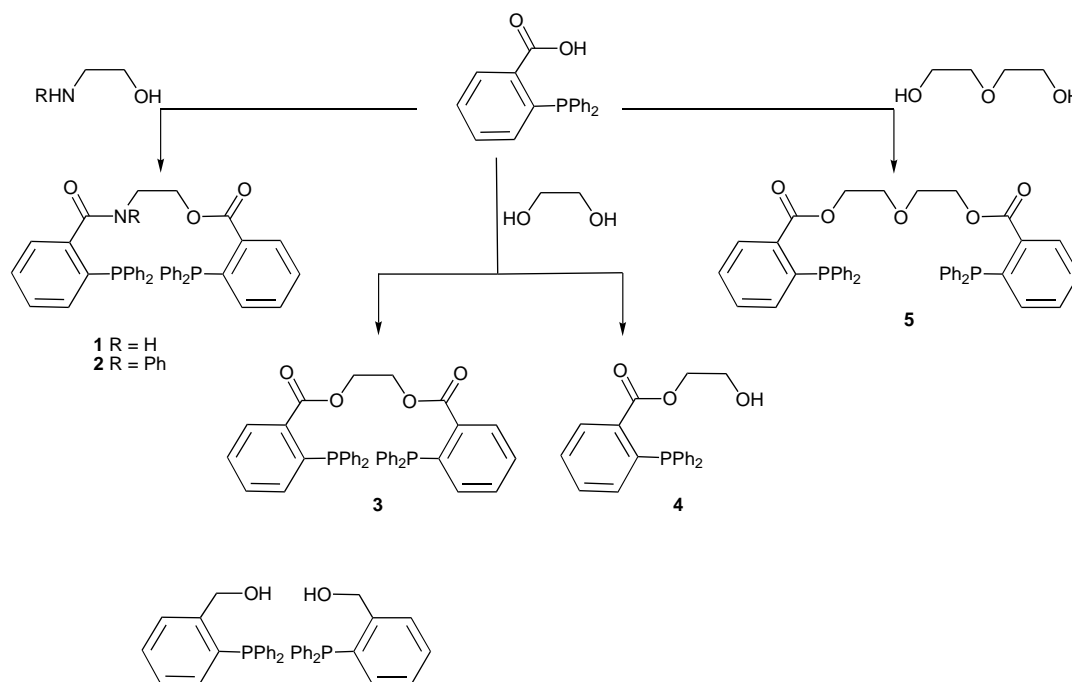
$[(\text{CH}_3)\text{Rh}(\text{CO})_2\text{I}_3]^-$ , so that catalyst design focuses on the improvement of this reaction.<sup>[8]</sup> Ligands that increase the electron density at the metal center should facilitate the oxidative addition step and, consequently, increase the overall rate of acetic acid formation.

For this purpose, a large variety of rhodium carbonyl complexes have been synthesized and tested for methanol carbonylation, giving comparable or better activities than the original Monsanto catalyst.<sup>[9–12]</sup> One of the most important classes of these active rhodium complexes is based on simple phosphine ligands such as  $\text{PEt}_3$ ,<sup>[13]</sup> or diphosphine ligands of the type  $\text{PPh}_2\text{---CH}_2\text{---CH}_2\text{---PPh}_2$ .<sup>[14]</sup> More recently, bidendate phosphorus–sulfur, phosphorus–oxygen and phosphorus–nitrogen ligands such as  $\text{PPh}_2\text{---CH}_2\text{---P}(\text{S})\text{Ph}_2$ ,<sup>[12]</sup>  $\text{PPh}_2\text{---CH}_2\text{---P}(\text{O})\text{Ph}_2$ ,<sup>[15]</sup> and  $\text{PPh}_2\text{---CH}_2\text{---P}(\text{NPh})\text{Ph}_2$ <sup>[11]</sup> have been shown to produce efficient catalysts with  $[\text{Rh}(\text{CO})_2\text{Cl}]_2$ .

However, attempts to modify the catalyst  $[\text{Rh}(\text{CO})_2\text{I}_2]^-$  and thus increase its activity by introducing electron-donating ligands are generally hampered by the instability of the

[a] Prof. Dr. G. Süß-Fink, C. M. Thomas, R. Mafua, Dr. B. Therrien<sup>+</sup>, Dr. E. Rusanov<sup>+</sup>, Prof. Dr. H. Stöckli-Evans<sup>+</sup>  
Institut de Chimie, Université de Neuchâtel, Case postale 2, 2007 Neuchâtel (Switzerland)  
Fax: (+41) 32-718-25-11  
E-mail: georg.suess-fink@unine.ch

[<sup>+</sup>] Crystal structure analysis.



Scheme 1. Synthesis of phosphine ligands **1–5** from 2-diphenylphosphinobenzoic acid.

complexes formed under the harsh reaction conditions required for the carbonylation of methanol. As iridium complexes are normally more stable than the corresponding rhodium complexes, efforts have been made to find suitable iridium catalysts for the carbonylation of methanol. This resulted in the development of the Cativa process, based on  $[\text{Ir}(\text{CO})_2\text{I}_2]^-$  in combination with  $[\text{Ru}(\text{CO})_4\text{I}_2]$ , which is presently the most efficient process for the industrial manufacture of acetic acid.<sup>[16]</sup>

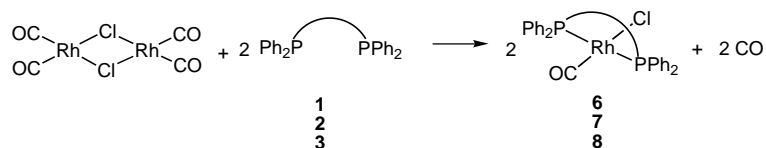
Herein we report on diphosphine ligands containing ethyleneglycol and amino alcohol spacer groups for the synthesis of *trans*-disubstituted square-planar rhodium and iridium complexes, which are not only active for methanol carbonylation but also robust under the catalytic conditions and thus recoverable intact.

## Results and Discussion

Square-planar rhodium complexes containing two monophosphine ligands in *trans* positions such as *trans*- $[(\text{PET}_3)_2\text{Rh}(\text{CO})\text{Cl}]^{[10]}$  are known to be highly active in the process of methanol carbonylation, but less stable than unsymmetrical diphosphine complexes such as *cis*- $[(\text{Ph}_2\text{PCH}_2\text{CH}_2\text{PAR}_2)\text{Rh}(\text{CO})\text{Cl}]^{[17]}$  which are, however, less active catalysts. For this reason, we decided to develop diphosphine ligands containing suitable spacer groups between the two phosphorus atoms in order to allow *trans* coordination in square-planar rhodium and iridium complexes. Complexes of this type can be expected to combine high catalytic activity with thermal stability under the harsh conditions of methanol carbonylation, so that they can be recovered intact after the catalytic process.

In general, easy accessibility is a major criterion for the design of new ligands. The ready availability of 2-diphenylphosphinobenzoic acid from the Wurtz coupling of sodium 2-chlorobenzoate and sodium diphenylphosphide<sup>[18]</sup> is an attractive building block for the synthesis of diphosphine ligands by condensation of the acid function with diols, diamines or amino alcohols.<sup>[19]</sup> Thus the new phosphine ligands **1–5** have been synthesized from 2-diphenylphosphinobenzoic acid and the corresponding amino alcohols or diols (Scheme 1). They can be isolated in good yields as white microcrystalline powders. Whereas the diphosphine ligands **3** and **5** are symmetrical and give only one resonance in the  $^{31}\text{P}\{^1\text{H}\}$  NMR spectrum, the diphosphine ligands **1** and **2** are unsymmetrical. However, only **2** gives rise to the expected two  $^{31}\text{P}$  signals, for **1** only one resonance is observed in the  $^{31}\text{P}\{^1\text{H}\}$  NMR spectrum. All spectroscopic data of **1–5** are given in the Experimental Section.

Complex  $[\{\text{Rh}(\text{CO})_2\text{Cl}\}_2]$  reacts with two equivalents of the diphosphines **1–3** to give the diphosphine complexes  $[(\text{P–P})\text{Rh}(\text{CO})\text{Cl}]$  **6–8**, respectively, in high yields (Scheme 2). The products are very easily isolated by evaporation of the solvent and washing of the residues with diethyl ether. Compounds **6–8** exhibit, as expected, one strong  $\nu(\text{CO})$  absorption in the IR spectrum, which is comparable with those reported for *trans*- $[(\text{PR}_3)_2\text{Rh}(\text{CO})\text{X}]$ ,<sup>[11, 13]</sup> but lower than that of the *cis*- $[(\text{dppe})\text{Rh}(\text{CO})\text{I}]$  (dppe = 1,2-bis(diphenylphosphino)ethane),<sup>[14]</sup> providing further evidence



Scheme 2. Synthesis of **6–8** from **1–3**, respectively.

for *trans* coordination. The monomeric nature of these complexes can be concluded from the mass spectra. All complexes show only one resonance for the two equivalent phosphorus atoms in the  $^{31}\text{P}\{^1\text{H}\}$  NMR spectrum, (see Experimental Section) which appears as a doublet due to coupling of the phosphorus atoms to  $^{103}\text{Rh}$  ( $I = 1/2$ ), in agreement with the *trans*-P,P stereochemistry. This is in line with the findings for the  $\alpha$ -cyclodextrin–diphosphine complexes developed by Matt and Armspach.<sup>[20]</sup> In the case of **7**, which contains the unsymmetrical diphosphine **2**, the  $^{31}\text{P}$  signal at  $\delta = 47.8$  ppm ( $J(^{103}\text{Rh}, ^{31}\text{P}) = 162$  Hz) observed at room temperature is a doublet. However, upon cooling to  $-60^\circ\text{C}$  ( $\text{CD}_2\text{Cl}_2$ ), this signal splits and the ABX pattern confirms the *trans* arrangement ( $J(^{31}\text{P}, ^{31}\text{P}) = 274$  Hz).

Several authors suggest that this type of mononuclear *trans* bidentate complex might be more stable with large metallacycles (13 atoms) than with medium-size metallacycles, due to the increased flexibility of the larger ring size.<sup>[21]</sup> In general, the stability of the *trans* monomer increases with increasing chain length and reaches a maximum with a metallacycle of 15 members.<sup>[22]</sup> In agreement with this statement, the complex  $[\{\text{Rh}(\text{CO})_2\text{Cl}\}_2]$  reacts with two equivalents of **5** (for which a mononuclear metallacycle containing 16 atoms is expected) to give the dinuclear complex  $[(\text{P}-\text{P})\text{Rh}(\text{CO})\text{Cl}]_2$  (**9**; Scheme 3).

The single-crystal X-ray structure analysis of **9** (Figure 1) shows that the two rhodium atoms are bridged by two diphosphine ligands, maintaining the *trans* P,P-coordination geometry of each rhodium atom. The molecule has a mirror plane passing through the Rh and Cl atoms. The two metal atoms are in a square-planar environment (Figure 1). The metal atoms are coordinated by the two P atoms of the two P,P-bidentate ligands. The four P–Rh bonds are equal in length (P(5a)–Rh(1) and P(5b)–Rh(2) = 2.345(2), P(6a)–Rh(1) and P(6b)–Rh(2) = 2.318(2) Å). These bond lengths and angles are similar to those reported by Shaw and co-workers<sup>[23]</sup> for *trans*- $\{[(t\text{Bu})_2\text{P}(\text{CH}_2)_{10}\text{P}(t\text{Bu})_2]\text{Rh}(\text{CO})\text{Cl}\}_2$  and *trans*- $\{[(t\text{Bu})_2\text{P}-(\text{CH}_2)_{10}\text{P}(t\text{Bu})_2]\text{PdCl}_2\}_2$ .

The chloro complexes  $[(\text{P}-\text{P})\text{Ir}(\text{cod})\text{Cl}]$  (**10**: P–P = **1**; **11**: P–P = **2**; **12**: P–P = **3**) are directly obtained from  $[\{\text{Ir}(\text{cod})\text{Cl}\}_2]$  and the corresponding diphosphine ligands using a 1:2 ratio in diluted solution to avoid the formation of  $[(\text{P}-\text{P})_2\text{Ir}]\text{Cl}$  or polynuclear species, as observed with other diphosphines

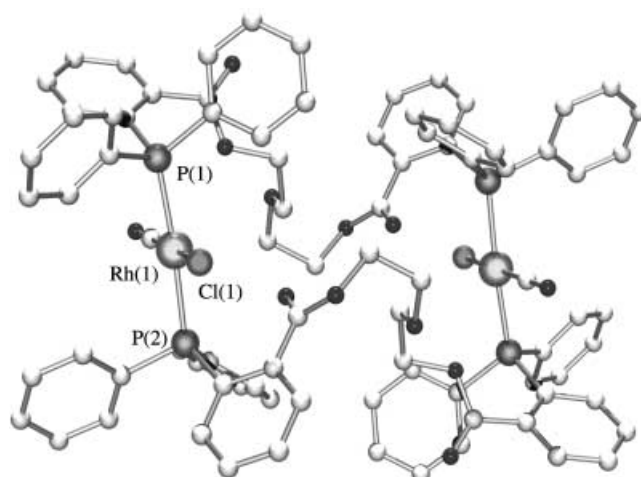
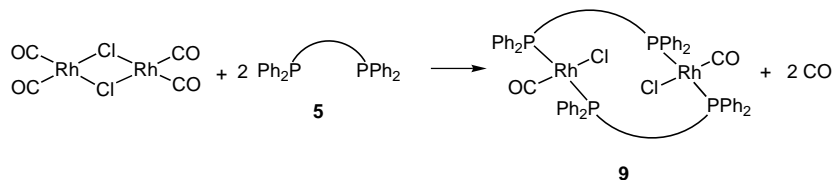
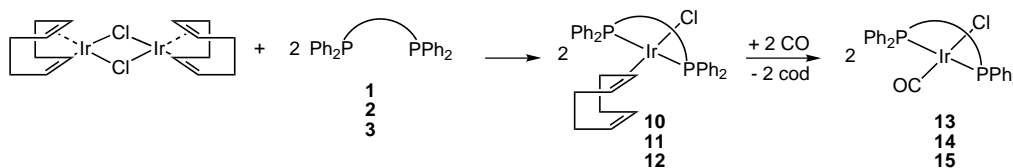


Figure 1. Molecular structure of **9**. Selected bond lengths [Å] and angles [ $^\circ$ ]: Rh(1)–P(5a) 2.345(2), Rh(1)–P(6a) 2.318(2), Rh(2)–P(5b) 2.345(2), Rh(2)–P(6b) 2.318(2); P(6)–Rh(1)–P(5) 175.24(5), C(21)–Rh(1)–Cl(1) 174.74(10), P(6)–Rh(1)–C(21) 90.33(9), C(21)–Rh(1)–P(5) 90.78(10), P(5)–Rh(1)–Cl(1) 91.74(9), Cl(1)–Rh(1)–P(6) 86.78(12).

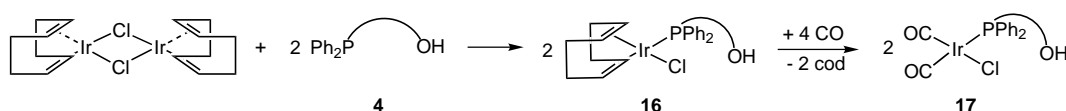
(Scheme 4).<sup>[24]</sup> The phosphorus atoms of the P–Ir–P moieties give rise to a signal at about  $\delta = 20.5$  ppm in the  $^{31}\text{P}\{^1\text{H}\}$  NMR spectrum. On the basis of the spectroscopic data (see Experimental Section), we can formally represent complexes  $[(\text{P}-\text{P})\text{Ir}(\text{cod})\text{Cl}]$  (**10**–**12**) as containing a monodentate cyclooctadiene ligand in a square-planar coordination geometry. In the  $^1\text{H}$  NMR spectrum the olefinic protons are distinctly different, the signal at  $\delta = 4.89$  ppm can be assigned to the noncoordinated  $\text{HC}=\text{CH}$  group, while the signal at  $\delta = 4.09$  ppm can be assigned to the coordinated  $\text{HC}=\text{CH}$  group. This is in line with the values for the corresponding group in free cod ( $\delta = 5.56$  ppm) and in  $[\{\text{Ir}(\text{cod})\text{Cl}\}_2]$  ( $\delta = 4.20$  ppm). However, a trigonal-bipyramidal coordination geometry with cod as a *cis*-bidentate ligand can not be ruled out completely as it was observed in  $[(\text{diop})\text{Ir}(\text{cod})\text{Cl}]$  (diop = isopropylidene-2,3-dihydroxy-1,4-bis(diphenylphosphino)butane)<sup>[25]</sup> or in  $[(\text{pnp})\text{Ir}(\text{cod})\text{Cl}]$  (pnp = ( $\alpha$ -methylbenzyl)bis(2-(diphenylphosphino)ethyl)amine).<sup>[26]</sup> In the latter cases, however, the diphosphine ligands diop and pnp are *cis*-coordinated to iridium, while in **10**–**12** the diphosphine ligands **1**–**3** are *trans*-coordinated. Carbon monoxide reacts in dichloromethane with **10**–**12** to give quantitatively the carbonyl complexes **13**–**15** (Scheme 4), which also show only one  $^{31}\text{P}\{^1\text{H}\}$  NMR resonance for the two equivalent phosphorus atoms but shifted to about 27.0 ppm.



Scheme 3. Reaction of  $[\{\text{Rh}(\text{CO})_2\text{Cl}\}_2]$  with **5** to give **9**.



Scheme 4. Synthesis of **10**–**12** and reaction with CO to give **13**–**15**, respectively.

Scheme 5. Synthesis of **16** and reaction with CO to give **17**.

The analogous reaction of the chlorooctadiene complex  $[\text{Ir}(\text{cod})\text{Cl}]_2$  with two equivalents of **4** in dichloromethane gives the iridium complex  $[(\text{4})\text{Ir}(\text{cod})\text{Cl}]$  (**16**) in good yield (Scheme 5). Complex **16** shows a broad signal at  $\delta = 20.3$  ppm in the  $^{31}\text{P}$  NMR spectrum. The single-crystal X-ray structure analysis of **16** (Figure 2) reveals a distorted square-planar coordination geometry of the iridium atom. Complex **16** contains a  $\text{Ir}-\text{Cl}\cdots\text{HO}$  hydrogen bonding interaction ( $\text{Ir}(1)-\text{H}(30)$  2.3209 Å;  $\text{Cl}(1)-\text{H}(30)-\text{O}(3)$  162.43°).

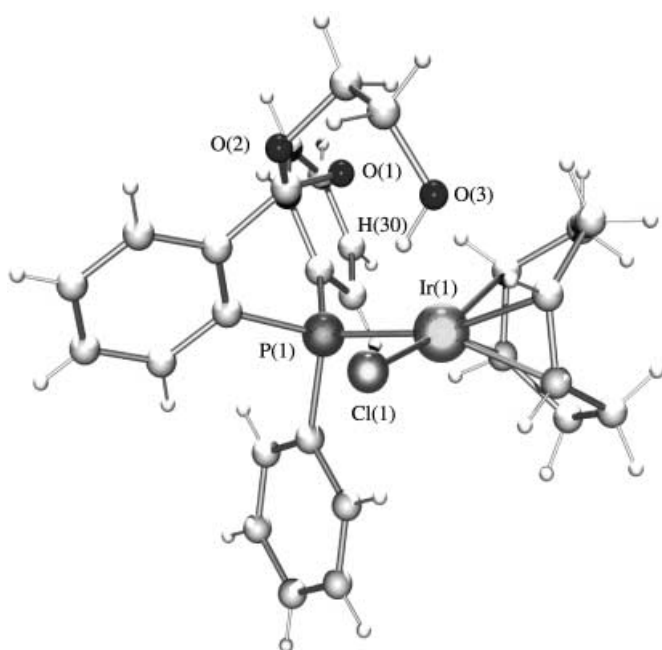
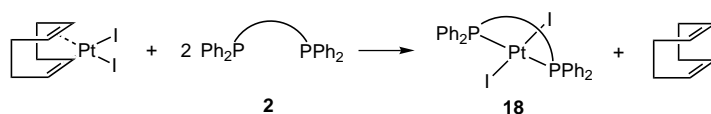


Figure 2. Molecular structure of **16**. Selected bond lengths [Å] and angles [°]:  $\text{Ir}(1)-\text{P}(1)$  2.342(18),  $\text{Ir}(1)-\text{C}(1)$  2.182(7),  $\text{Ir}(1)-\text{C}(4)$  2.108(7),  $\text{Ir}(1)-\text{C}(8)$  2.154(7),  $\text{Ir}(1)-\text{Cl}(1)$  2.379(16);  $\text{P}(1)-\text{Ir}(1)-\text{C}(8)$  164.8(2),  $\text{P}(1)-\text{Ir}(1)-\text{C}(1)$  158.2(2),  $\text{C}(4)-\text{Ir}(1)-\text{Cl}(1)$  155.8(2),  $\text{C}(5)-\text{Ir}(1)-\text{Cl}(1)$  164.4(2),  $\text{P}(1)-\text{Ir}(1)-\text{Cl}(1)$  90.7(6).

The *trans* coordination of the diphosphine ligands in the mononuclear complexes, assumed for **6–8**, **10–12**, and **13–15** on the basis of their spectroscopic data, was finally evidenced for the platinum complex  $[(\text{2})\text{PtI}_2]$  (**18**). Complex **18** is obtained almost quantitatively by the reaction of  $[\text{Pt}(\text{cod})\text{I}_2]$  with the diphosphine ligand (**2**) in dichloromethane (Scheme 6). In the  $^{31}\text{P}\{^1\text{H}\}$  NMR spectrum, the two inequivalent phosphorus atoms give rise to two very close signals at  $\delta = 12.1$  ppm and  $\delta = 11.6$  ppm, showing the characteristic

Scheme 6. Synthesis of **18**.

satellites due to  $^{31}\text{P}-^{195}\text{Pt}$  coupling. In the  $^1\text{H}$  NMR spectrum, **18** gives rise to the expected signals of ligand **2**.

The *trans* coordination of **2** in **18** is unambiguously revealed by a single-crystal X-ray structure analysis (Figure 3) showing a square-planar coordination geometry of **18**. The Pt atom is coordinated to two I atoms and to the two P atoms of the diphosphine ligand. The two platinum–phosphorus bonds ( $\text{Pt}(1)-\text{P}(1)$ , 2.313(9);  $\text{Pt}(1)-\text{P}(2)$ , 2.335(9) Å) and the two platinum–iodine bonds ( $\text{Pt}(1)-\text{I}(1)$  2.610(5);  $\text{Pt}(1)-\text{I}(2)$

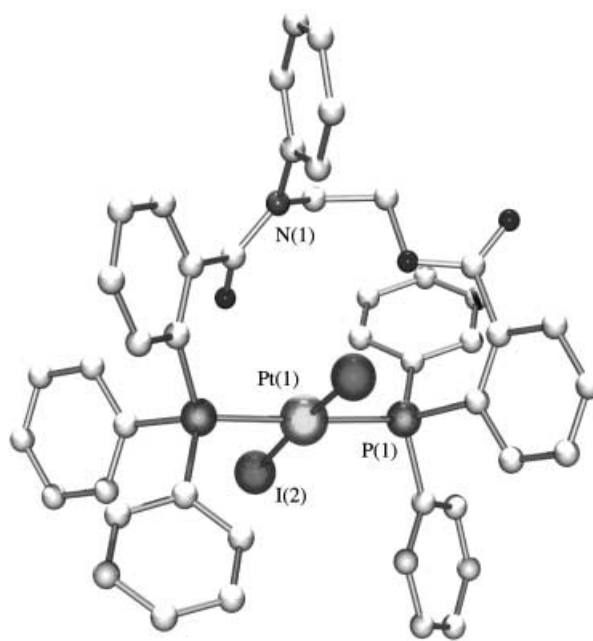


Figure 3. Molecular structure of **18**. Selected bond lengths [Å] and angles [°]:  $\text{Pt}(1)-\text{P}(1)$  2.313(9),  $\text{Pt}(1)-\text{P}(2)$  2.335(9),  $\text{Pt}(1)-\text{I}(1)$  2.610(5),  $\text{Pt}(1)-\text{I}(2)$  2.615(5);  $\text{P}(1)-\text{Pt}(1)-\text{P}(2)$  178.40(4),  $\text{P}(1)-\text{Pt}(1)-\text{I}(1)$  93.52(3),  $\text{P}(1)-\text{Pt}(1)-\text{I}(2)$  89.29(3),  $\text{P}(2)-\text{Pt}(1)-\text{I}(2)$  86.05(3),  $\text{P}(2)-\text{Pt}(1)-\text{I}(2)$  91.30(3),  $\text{I}(1)-\text{Pt}(1)-\text{I}(2)$  173.22(10).

2.62(5) Å) are almost equal in length. These bond lengths are similar to those reported by Feringa and co-workers for *trans*-dichloro[bis(*N*-(2-diphenylphosphino)phenyl)-2,6-pyridinedicarboxamide]platinum.<sup>[27]</sup> The angles about the platinum center in **18** are not far from those of the ideal square-planar geometry.

The diphosphine ligands **1**, **2**, **3**, and **5** have been tested in combination with  $[\text{Rh}(\text{CO})_2\text{Cl}]_2$  or  $[\text{Ir}(\text{cod})\text{Cl}]_2$  for the catalytic carbonylation of methanol to give acetic acid and methyl acetate in the presence of iodomethane and water. The reaction was carried out at 170 °C under a CO pressure of 22 bar, the catalyst:substrate ratio being 1:2000. After

15 min the reaction was stopped, and the products were analyzed by GC to determine the quantities formed. The results of the catalytic carbonylation of methanol are presented in Table 1. As a control experiment, the catalytic reaction was carried out with the Monsanto catalyst  $[\text{Rh}(\text{CO})_2\text{I}_2]^-$ , which was formed in situ from  $[\{\text{Rh}(\text{CO})_2\text{Cl}\}_2]$  under the reaction conditions (Table 1, entry 1).<sup>[12]</sup> In the presence of the diphosphines **1**–**5**, the IR spectra showed the absence of the intense  $\nu(\text{CO})$  bands for  $[\text{Rh}(\text{CO})_2\text{I}_2]^-$ . As shown in Table 1, the catalytic activity increases considerably in the presence of the diphosphine ligands **1**, **2**, **3**, or **5**, ligand **2** being the most active (Table 1, entry 3).

Table 1. Methanol carbonylation data.<sup>[a]</sup>

Entry	Precursor	Ligand	TON <sup>[b]</sup>
1	$[\{\text{Rh}(\text{CO})_2\text{Cl}\}_2]$	–	381
2	$[\{\text{Rh}(\text{CO})_2\text{Cl}\}_2]$	<b>1</b>	732
3	$[\{\text{Rh}(\text{CO})_2\text{Cl}\}_2]$	<b>2</b>	803
4	$[\{\text{Rh}(\text{CO})_2\text{Cl}\}_2]$	<b>3</b>	672
5	residue from entry 3	–	781
6	$[\{\text{Rh}(\text{CO})_2\text{Cl}\}_2]$	<b>5</b>	650
7	$[\{\text{Ir}(\text{cod})\text{Cl}\}_2]$	–	227
8	$[\{\text{Ir}(\text{cod})\text{Cl}\}_2]$	<b>1</b>	312
9	$[\{\text{Ir}(\text{cod})\text{Cl}\}_2]$	<b>2</b>	350
10	$[\{\text{Ir}(\text{cod})\text{Cl}\}_2]$	<b>3</b>	321
11	$[\{\text{Ir}(\text{cod})\text{Cl}\}_2]/[\text{Ru}(\text{CO})_4\text{I}_2]$	–	612

[a] Catalytic conditions:  $[\{\text{Rh}(\text{CO})_2\text{Cl}\}_2]$  or  $[\{\text{Ir}(\text{cod})\text{Cl}\}_2]$  (57  $\mu\text{mol}$ ), ligand (0.12 mmol, 2 equiv),  $\text{CH}_3\text{OH}$  (110.2 mmol),  $\text{CH}_3\text{I}$  (11.4 mmol),  $\text{H}_2\text{O}$  (81.9 mmol), 170 °C, 22 bar, 900 rpm, reaction time = 15 min. [b] mol  $\text{CH}_3\text{OH}$  converted into  $\text{CH}_3\text{COOH}$  and  $\text{CH}_3\text{COOCH}_3$  per mol catalyst precursor.

In the case of the most active combination,  $[\{\text{Rh}(\text{CO})_2\text{Cl}\}_2]/$  ligand **2**, the catalyst stays active throughout several catalytic runs. A homogeneous orange-red solution is obtained after the catalytic reaction, containing three rhodium–diphosphine complexes. By IR and  $^{31}\text{P}$  NMR analysis, one of them is identified as the rhodium(I) complex **7** (80 %) ( $\delta = 47.8$  ppm,  $^1J(^{103}\text{Rh}, ^{31}\text{P}) = 164$  Hz,  $\nu(\text{CO}) = 1970$   $\text{cm}^{-1}$ ), the other is the rhodium(III) complex **19** (15 %) ( $\delta = 30.8$  ppm,  $^1J(^{103}\text{Rh}, ^{31}\text{P}) = 100$  Hz); a third minor species (5 %;  $\nu(\text{CO}) = 2040$   $\text{cm}^{-1}$ ) has not, so far, been identified. This mixture is still active for further catalytic runs, showing almost the same degree of catalytic activity. There is no evidence for ligand degradation by hydrolysis of the amide or ester bonds nor by quaternization of the phosphine units by methyl iodide.

The red complex **19** can be isolated from the organometallic residue of the catalytic reaction by crystallization from acetone; it is also directly accessible from the reaction of **7** with methyl iodide in acetone solution (Scheme 7). Complex **19** is a dinuclear  $\text{Rh}^{\text{III}}$  complex in which the rhodium atoms are bridged by one diphosphine and two iodo ligands, both

rhodium atoms carrying an acetyl ligand. Complex **19** exists in two isomers **19a** and **19b**, depending on the *cis* or *trans* arrangement of the two terminal iodo ligands at the two rhodium atoms. The two isomers present in solution are separated by fractional crystallization from acetone: **19a** crystallizes rapidly, while **19b** takes several hours to crystallize after elimination of **19a**. The structures of **19a** and **19b** are shown in Figures 4 and 5, respectively. The Rh–COMe bond

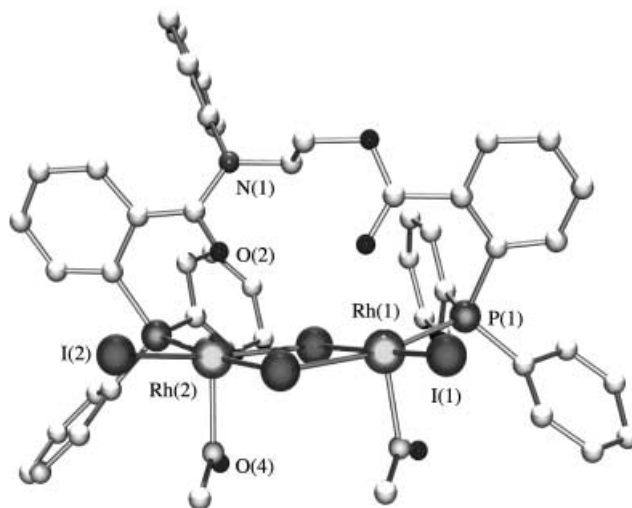


Figure 4. Molecular structure of **19a**. Selected bond lengths [ $\text{\AA}$ ] and angles [ $^\circ$ ]: Rh(1)–P(1) 2.274(7), Rh(2)–P(2) 2.278(7), Rh(1)–O(1) 2.330(18), Rh(2)–O(2) 2.294(18), Rh(1)–C(47) 2.15(3), Rh(2)–C(49) 2.11(3); C(47)–Rh(1)–O(1) 174.2(8), I(4)–Rh(1)–I(1) 171.64(11), P(1)–Rh(1)–I(3) 168.7(2), C(49)–Rh(2)–O(2) 175.1(8), I(2)–Rh(2)–I(4) 168.04(12), P(2)–Rh(2)–I(3) 173.9(3).

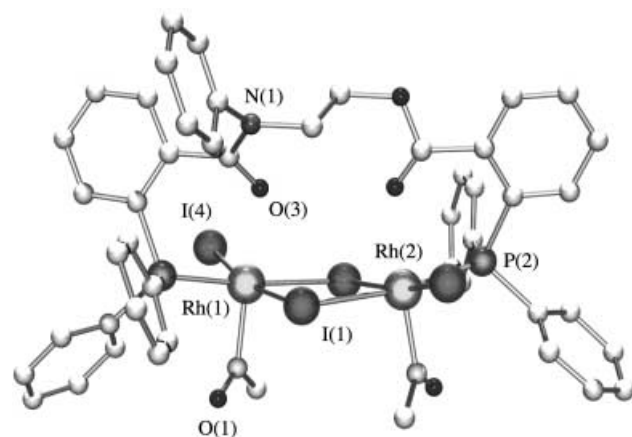
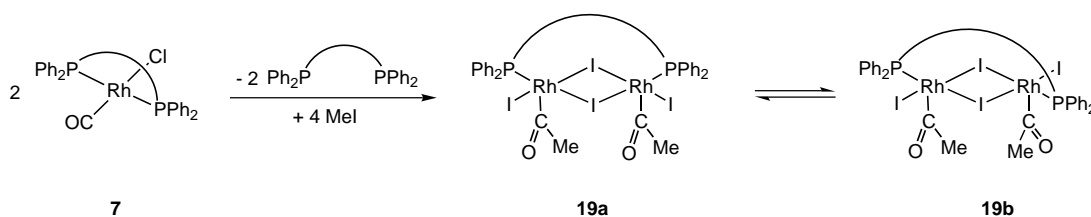
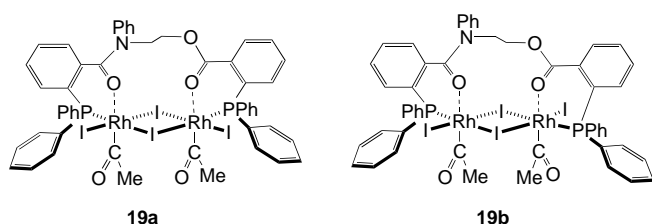


Figure 5. Molecular structure of **19b**. Selected bond lengths [ $\text{\AA}$ ] and angles [ $^\circ$ ]: Rh(1)–P(1) 2.280(3), Rh(2)–P(2) 2.273(2), Rh(1)–O(5) 2.388(7), Rh(2)–O(3) 2.334(6), Rh(1)–C(1) 1.996(11), Rh(2)–C(3) 2.02(12); C(1)–Rh(1)–O(5) 167.0(4), I(4)–Rh(1)–I(1) 166.63(4), P(1)–Rh(1)–I(2) 170.65(8), C(3)–Rh(2)–O(3) 173.4(4), I(2)–Rh(2)–I(3) 167.82(4), P(2)–Rh(2)–I(1) 173.77(7).

Scheme 7. Reactions of **7** with methyl iodide.

lengths of **19a** are relatively long, 2.11 and 2.15 Å, as compared with the corresponding bonds in most other rhodium acetyl complexes, which generally have bond lengths around 2.00 Å (Figure 4). The same is true for **19b** (1.99 and 2.02 Å; Figure 5). The long Rh–COMe bond must reflect a large *trans* influence of the carbonyl groups of the ligand. As a consequence, the Rh–O bonds in **19a** (2.33 and 2.29 Å) are shorter than those observed for **19b** (2.33 and 2.38 Å). The geometry of the six-membered chelate ring formed by these Rh–O interactions can explain the relative stability of the two complexes and more generally of the catalytic system. In the case of **19a**, the acetyl ligands have the same orientation, the acetyl oxygen atoms pointing towards the hydrogen atom of a phenyl group because there is an intramolecular contact between these two atoms (2.59 and 2.61 Å). In **19b**, the acetyl groups also form hydrogen bonds (2.46 and 2.65 Å) and for this reason show an opposite orientation as shown in Scheme 8.



Scheme 8. Isomers **19a** and **19b** showing the Rh–O interactions which complete the octahedral coordination geometry at the two Rhodium atoms.

It is noteworthy that in both isomers **19a** and **19b**, the rhodium atoms do not have a square-pyramidal but an octahedral coordination geometry, thanks to the carbonyl oxygen atoms of the ligand chain (Rh–O 2.33 and 2.29 Å in **19a**, 2.33 and 2.38 Å in **19b**). The six-membered chelating ring is approximately planar, the two Rh–P bonds (2.28 and 2.27 Å) are equal in length for **19a** and **19b**.

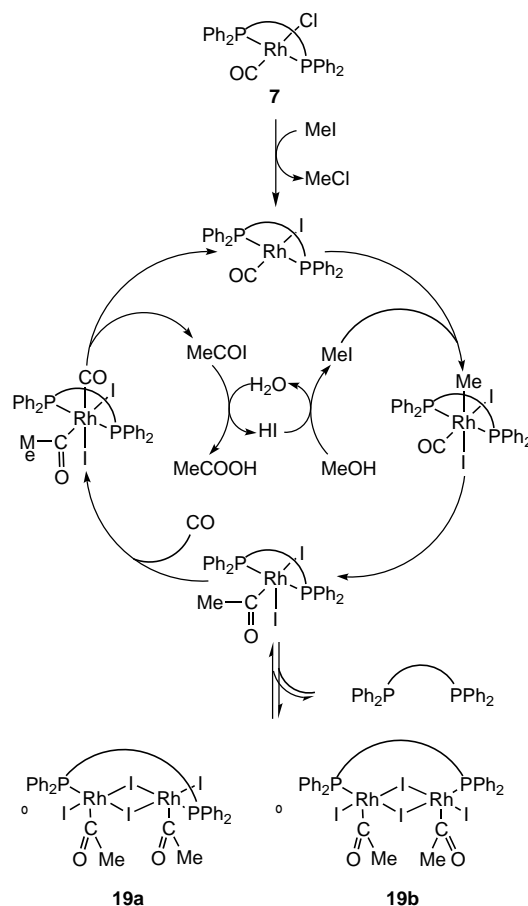
## Conclusion

Pringle et al. have supposed<sup>[17]</sup> that the asymmetry of the diphosphine ligand is a very important factor in the catalytic activity and the stability of the rhodium complex in the carbonylation of methanol, as has been shown by Casey et al. for the rhodium–phosphine catalyzed hydroformylation of olefins.<sup>[28]</sup> Indeed, the rhodium complex **7**, containing an asymmetric diphosphine ligand, turned out to be more active and more stable under catalytic conditions than the classical Monsanto system.

During the formation of the dinuclear complex **19** from two mononuclear complexes **7**, one of the two diphosphine ligands is liberated. Phosphine loss during the catalytic process has already been proposed by Cole-Hamilton et al. in the case of  $[(\text{PEt}_3)_2\text{Rh}(\text{CO})\text{I}]$ , without the supposed monophosphine species  $[(\text{PEt}_3)\text{Rh}(\text{CO})\text{I}]$  being isolated.<sup>[13]</sup> Oxidative addition of iodomethane to **7** yields the acetylrhodium(III) complex **19**, presumably through the intermediacy of the corresponding mononuclear methylrhodium(III) complex. The facile migra-

tory insertion of carbon monoxide during oxidative addition of iodomethane to carbonylrhodium(I) complexes is well known.<sup>[29, 30]</sup>

On the basis of these observations, we propose the catalytic cycle shown in Scheme 9 for the mechanism of the carbonylation of methanol catalyzed by **7**. Alternatively, it is possible that the proposed hexacoordinate methyl and acetyl species



Scheme 9. Catalytic cycle showing the mechanism of the carbonylation of methanol catalysed by **7**.

$[(\text{Me})\text{Rh}(\mathbf{19})\text{I}_2]$  and  $[(\text{COMe})\text{Rh}(\mathbf{19})\text{I}_2]$  represent in reality pentacoordinate cations  $[(\text{Me})\text{Rh}(\mathbf{19})\text{I}]^+$  and  $[(\text{COMe})\text{Rh}(\mathbf{19})\text{I}]^+$  with  $\text{I}^-$  counterions. A similar cycle has been proposed for the reaction catalyzed by  $[(\text{Ph}_2\text{PCH}_2\text{PSPH}_2)\text{Rh}(\text{CO})\text{I}]$ , in which several intermediates have been detected by spectroscopy.<sup>[12]</sup> The dinuclear complexes **19** formed by elimination of a diphosphine ligand may be considered as a reservoir for the mononuclear active species. The formation of the dinuclear complex **19** can be decreased by using an excess of the diphosphine ligand.

## Experimental Section

**General:** Solvents were dried and distilled under nitrogen prior to use. All reactions were carried out under nitrogen, using standard Schlenk techniques. All other reagents were purchased (Fluka) and used as received. Nuclear magnetic resonance spectra were recorded using a Varian Gemini 200BB instrument and referenced to the signals of the

residual protons in the deuterated solvents.  $^1\text{H}$  NMR: internal standard solvent, external standard TMS;  $^{13}\text{C}$  NMR: internal standard solvent, external standard TMS. IR spectra were recorded with a Perkin–Elmer 1720X FTIR spectrometer. Microanalyses were carried out by the Laboratory of Pharmaceutical Chemistry, University of Geneva, Switzerland.

**1:** A solution of 2-diphenylphosphinobenzoic acid (1 g, 3.26 mmol), *N,N*-dicyclohexylcarbodiimide (2.7 g, 13.05 mmol), 4-(dimethylamino)pyridine (100 mg, 0.82 mmol), 4-pyrrolidinopyridine (100 mg, 0.68 mmol), and ethanolamine (0.1 mL, 1.62 mmol) in  $\text{CH}_2\text{Cl}_2$  (40 mL) was allowed to stand at room temperature under nitrogen, until esterification was complete. The resulting solution was filtered through Celite to remove *N,N*-dicyclohexyl urea, and the filtrate concentrated under reduced pressure. A chromatogram of the residue was recorded on a silica gel column (150 g), eluting with hexane/acetone (2:1). The product was isolated from the third fraction by evaporation of the solvent, giving **1** (220 mg, 0.33 mmol; 20%) as a white solid.  $^1\text{H}$  NMR (200 MHz,  $[\text{D}_6]\text{acetone}$ , 21 °C):  $\delta$  = 8.41 (s, 1H; –NH), 7.50–7.19 (m, 28H; ArH), 3.87–3.75 (m, 2H; –OCH<sub>2</sub>–), 3.47–3.41 ppm (m, 2H; N–CH<sub>2</sub>–);  $^{13}\text{C}$  NMR (50 MHz,  $[\text{D}_6]\text{acetone}$ , 21 °C):  $\delta$  = 170.73, 153.77, 144.90, 144.55, 137.74–126.10, 68.71, 49.81 ppm;  $^{31}\text{P}$  NMR (81 MHz,  $[\text{D}_6]\text{acetone}$ , 21 °C):  $\delta$  = –12.47 ppm (brs); IR (KBr):  $\tilde{\nu}$  = 3283 m, 3071 vw, 3050 vw, 3002 vw, 2927 s, 2852 m, 2119 vw, 1695 vs (C=O ester), 1645 s (C=O amide), 1584 vw, 1519 s, 1432 m, 1349 m, 1119 m, 748 m, 694 m cm<sup>–1</sup>; ESI-MS:  $m/z$ : 637 [ $M^+$ ]; elemental analysis calcd (%) for  $\text{C}_{40}\text{H}_{33}\text{N}_1\text{O}_3\text{P}_2$  (637.6): C 75.3, H 5.2; found: C 75.1, H 5.3.

**2:** A solution of 2-diphenylphosphinobenzoic acid (1.12 g, 3.65 mmol), *N,N*-dicyclohexylcarbodiimide (900 mg, 4.36 mmol), 4-(dimethylamino)pyridine (100 mg, 0.82 mmol), 4-pyrrolidinopyridine (100 mg, 0.68 mmol), and *N*-(2-hydroxyethyl)aniline (0.18 mL, 1.47 mmol) in  $\text{CH}_2\text{Cl}_2$  (50 mL) was allowed to stand at room temperature under nitrogen, until esterification was complete. The resulting solution was filtered through Celite to remove *N,N*-dicyclohexylurea, and the filtrate concentrated under reduced pressure. A chromatogram of the residue was recorded on a silica gel column (150 g), eluting with hexane/diethyl ether (1:1). The product was isolated from the third fraction by evaporation of the solvent, giving **2** (483 mg, 0.68 mmol; 46%) as a white solid.  $^1\text{H}$  NMR (200 MHz,  $[\text{D}_6]\text{DMSO}$ , 21 °C):  $\delta$  = 7.88–6.81 (m, 33H; ArH), 4.34 (br, 2H; –OCH<sub>2</sub>–), 4.16 ppm (br, 2H; –NCH<sub>2</sub>–);  $^{13}\text{C}$  NMR (50 MHz,  $[\text{D}_6]\text{DMSO}$ , 21 °C):  $\delta$  = 170.42, 166.54, 144.31–140.45, 138.40–137.66, 134.85–127.97, 63.04, 48.59 ppm;  $^{31}\text{P}$  NMR (81 MHz,  $[\text{D}_6]\text{DMSO}$ , 21 °C):  $\delta$  = –4.84 (s, phosphorus ester), –12.22 ppm (s, phosphorus amide); IR (KBr):  $\tilde{\nu}$  = 3441 vw, 3053 vw, 2927 vw, 2852 vw, 1717 s (C=O ester), 1650 s (C=O amide), 1586 vw, 1494 w, 1434 m, 1268 m, 1253 s, 1141 vw, 1111 w, 745 s, 697 vs cm<sup>–1</sup>; ESI-MS:  $m/z$ : 736 [ $M+\text{Na}^+$ ]; elemental analysis calcd (%) for  $\text{C}_{46}\text{H}_{37}\text{N}_1\text{O}_3\text{P}_2$  (713.7): C 77.4, H 5.2; found: C 76.9, H 5.4.

**3 and 4:** A solution of 2-diphenylphosphinobenzoic acid (1 g, 3.26 mmol), *N,N*-dicyclohexylcarbodiimide (2.7 g, 13.05 mmol), 4-(dimethylamino)pyridine (100 mg, 0.82 mmol), 4-pyrrolidinopyridine (100 mg, 0.68 mmol), and ethyleneglycol (0.09 mL, 1.61 mmol) in  $\text{CH}_2\text{Cl}_2$  (50 mL) was allowed to stand at room temperature under nitrogen, until esterification was complete. The resulting solution was filtered through Celite to remove *N,N*-dicyclohexylurea, and the filtrate concentrated under reduced pressure. A chromatogram of the residue was recorded on a silica gel column (150 g), eluting with hexane/diethyl ether (1:1). The products were isolated from the second (**4**) and the third (**3**) fractions, giving **3** (772 mg, 1.21 mmol; 75%) and **4** (100 mg, 0.31 mmol; 19%) as white solids. Analytical data for **3**:  $^1\text{H}$  NMR (200 MHz,  $\text{CDCl}_3$ ):  $\delta$  = 8.10–7.20 (m, 28H; ArH), 4.31 (t, 2H; –OCH<sub>2</sub>–), 3.72 ppm (t, 2H; –OCH<sub>2</sub>–);  $^{13}\text{C}$  NMR (50 MHz,  $\text{CDCl}_3$ ):  $\delta$  = 167.59, 157.55, 139.06–125.04, 67.64, 61.16 ppm;  $^{31}\text{P}$  NMR (81 MHz,  $\text{CDCl}_3$ ):  $\delta$  = –4.21 ppm (brs); IR (KBr):  $\tilde{\nu}$  = 3325 w, 3052 w, 2928 m, 2850 m, 1715 vs (C=O ester), 1626 m, 1584 w, 1435 s, 1270 vs, 1254 vs, 1117 m, 1056 s, 989 w, 746 vs, 696 vs cm<sup>–1</sup>; ESI-MS:  $m/z$ : 639 [ $M^+$ ]; elemental analysis calcd (%) for  $\text{C}_{40}\text{H}_{32}\text{O}_3\text{P}_2$  (638.6): C 75.2, H 5.0; found: C 75.4, H 5.4. Analytical data for **4**:  $^1\text{H}$  NMR (200 MHz,  $\text{CDCl}_3$ , 21 °C):  $\delta$  = 8.10–6.92 (m, 14H; ArH), 4.32 (s, 1H; –OH), 3.95–3.87 (m, 2H; –OCH<sub>2</sub>–), 3.52–3.48 ppm (m, 2H; –C(O)OCH<sub>2</sub>–);  $^{13}\text{C}$  NMR (50 MHz,  $\text{CDCl}_3$ , 21 °C):  $\delta$  = 166.80, 154.19, 140.91, 138.30, 135.22–128.67, 63.21, 50.21 ppm;  $^{31}\text{P}$  NMR (81 MHz,  $\text{CDCl}_3$ , 21 °C):  $\delta$  = –3.71 ppm (brs); IR (KBr):  $\tilde{\nu}$  = 3328 br, 2928 w, 1708 vs (C=O ester), 1627 m, 1582 w, 1462 vw, 1437 m, 1271 vs, 1141 m, 1109 m, 1057 s, 749 s, 699 vs cm<sup>–1</sup>; ESI-MS:  $m/z$ : 350 [ $M^+$ ];

elemental analysis calcd (%) for  $\text{C}_{21}\text{H}_{19}\text{O}_3\text{P}_1$  (350.3): C 72.0, H 5.5; found: C 72.4, H 5.4.

**5:** A solution of 2-diphenylphosphinobenzoic acid (1 g, 3.26 mmol), *N,N*-dicyclohexylcarbodiimide (2.7 g, 13.05 mmol), 4-(dimethylamino)pyridine (100 mg, 0.82 mmol), 4-pyrrolidinopyridine (100 mg, 0.68 mmol), and diethyleneglycol (0.16 mL, 1.63 mmol) in  $\text{CH}_2\text{Cl}_2$  (50 mL) was allowed to stand at room temperature under nitrogen, until esterification was complete. The resulting solution was filtered through Celite to remove *N,N*-dicyclohexyl urea, and the filtrate concentrated under reduced pressure. A chromatogram of the residue was recorded on a silica gel column (150 g), eluting with hexane/diethyl ether (1:1). The product was isolated from the third fraction by evaporation of the solvent, giving **5** (567 mg, 0.82 mmol; 51%) as a white solid.  $^1\text{H}$  NMR (200 MHz,  $\text{CDCl}_3$ , 21 °C):  $\delta$  = 8.20–6.89 (m, 28H; ArH), 4.31 (t, 4H; –OCH<sub>2</sub>–), 3.60 ppm (t, 4H; C(CO)OCH<sub>2</sub>–);  $^{13}\text{C}$  NMR (50 MHz,  $\text{CDCl}_3$ , 21 °C):  $\delta$  = 167.92, 140.93, 140.43, 138.24, 138.03, 134.602–133.73, 132.27, 131.08, 131.03, 129.16–128.51, 69.08, 64.42 ppm;  $^{31}\text{P}$  NMR (81 MHz,  $\text{CDCl}_3$ , 21 °C):  $\delta$  = –3.91 ppm (brs); IR (KBr):  $\tilde{\nu}$  = 3431 m, 3054 vw, 2928 w, 2875 w, 1718 vs (C=O ester), 1650 vw, 1584 vw, 1479 vw, 1434 m, 1270 s, 1254 vs, 1117 s, 1056 m, 989 vw, 746 s, 696 s cm<sup>–1</sup>; ESI-MS:  $m/z$ : 705 [ $M+\text{Na}^+$ ]; elemental analysis calcd (%) for  $\text{C}_{42}\text{H}_{36}\text{O}_5\text{P}_2$  (682.7): C 73.9, H 5.3; found: C 73.6, H 5.6.

**6:** A solution of  $[\{\text{Rh}(\text{CO})_2\text{Cl}\}_2]$  (50 mg, 0.13 mmol) and **1** (89 mg, 0.14 mmol) in dichloromethane (20 mL) was stirred at room temperature for 2 h. The solvent was then removed under reduced pressure. The residue was dissolved in acetone (10 mL), filtered, then evaporated to dryness. The resulting yellow solid was washed with hexane (10 mL) and dried in vacuo (62 mg, 0.08 mmol, 62%).  $^1\text{H}$  NMR (200 MHz,  $[\text{D}_6]\text{acetone}$ , 21 °C):  $\delta$  = 8.13 (s, 1H; –NH), 7.72–7.19 (m, 28H; ArH), 3.98–3.67 (m, 2H; –OCH<sub>2</sub>–), 3.52–3.41 ppm (m, 2H, N–CH<sub>2</sub>–);  $^{13}\text{C}$  NMR (50 MHz,  $[\text{D}_6]\text{acetone}$ , 21 °C):  $\delta$  = 171.25, 153.62, 144.80, 144.42, 138.54–125.20, 68.62, 49.92 ppm;  $^{31}\text{P}$  NMR (81 MHz,  $[\text{D}_6]\text{acetone}$ , 21 °C):  $\delta$  = 35.2 ppm (d,  $^1J(^{103}\text{Rh}, ^{31}\text{P}) = 159$  Hz); IR (KBr):  $\tilde{\nu}$  = 3441 m, 2926 m, 2852 w, 1981 vs, 1698 vs (C=O ester), 1645 vs (C=O amide), 1585 w, 1494 vw, 1435 s, 1277 s, 1092 m, 748 m, 697 vs cm<sup>–1</sup>; ESI-MS:  $m/z$ : 844 [ $M^+$ ]; elemental analysis calcd (%) for  $\text{C}_{47}\text{H}_{37}\text{Cl}_1\text{N}_1\text{O}_4\text{P}_2\text{Rh}_1$  (804.0): C 61.2, H 4.1; found: C 61.5, H 4.3.

**7:** A solution of  $[\{\text{Rh}(\text{CO})_2\text{Cl}\}_2]$  (50 mg, 0.13 mmol) and **2** (100 mg, 0.14 mmol) in dichloromethane (20 mL) was stirred at room temperature for 2 h. The solvent was then removed under reduced pressure. The residue was dissolved in acetone (10 mL), filtered, then evaporated to dryness. The resulting yellow solid was washed with hexane (10 mL) and dried in vacuo (71 mg, 0.08 mmol, 62%).  $^1\text{H}$  NMR (200 MHz,  $\text{CDCl}_3$ , 21 °C):  $\delta$  = 8.03–6.25 (m, 33; ArH), 4.73–4.71 (br, 2H; –OCH<sub>2</sub>–), 4.24–3.51 ppm (br, 2H; –NCH<sub>2</sub>–);  $^{13}\text{C}$  NMR (50 MHz,  $\text{CDCl}_3$ , 21 °C):  $\delta$  = 170.42, 166.54, 144.31–140.45, 138.40–137.66, 134.85–127.97, 63.04, 48.59 ppm;  $^{31}\text{P}$  NMR (81 MHz,  $\text{CDCl}_3$ , –60 °C):  $\delta$  = 45.1 (dd,  $^1J(^{103}\text{Rh}, ^{31}\text{P}) = 164$  Hz,  $^2J(^{31}\text{P}, ^{31}\text{P}) = 274$  Hz), 46.9 ppm (m); IR (KBr):  $\tilde{\nu}$  = 3441 m, 2926 m, 2852 w, 1971 vs, 1718 s (C=O ester), 1627 vs (C=O amide), 1585 w, 1494 vw, 1435 s, 1277 s, 1092 m, 747 m, 697 vs cm<sup>–1</sup>; ESI-MS:  $m/z$ : 844 [ $M^+ - \text{Cl}$ ]; elemental analysis calcd (%) for  $\text{C}_{47}\text{H}_{37}\text{Cl}_1\text{N}_1\text{O}_4\text{P}_2\text{Rh}_1$  (880.1): C 64.1, H 4.2; found: C 64.5, H 4.3.

**8:** A solution of  $[\{\text{Rh}(\text{CO})_2\text{Cl}\}_2]$  (50 mg, 0.13 mmol) and **3** (240 mg, 0.38 mmol) in acetonitrile (20 mL) was stirred at room temperature for 2 h. The solution was filtered then evaporated to dryness. The resulting yellow solid was washed with diethyl ether (3 × 10 mL) and dried in vacuo (97 mg, 0.12 mmol, 92%).  $^1\text{H}$  NMR (200 MHz,  $\text{CD}_2\text{Cl}_2$ , 21 °C):  $\delta$  = 8.02–6.75 (m, 28H; ArH), 4.32 (t, 2H; –OCH<sub>2</sub>–), 4.32 (t, 2H; –OCH<sub>2</sub>–), 3.98 ppm (t, 2H; –OCH<sub>2</sub>–);  $^{13}\text{C}$  NMR (50 MHz,  $\text{CD}_2\text{Cl}_2$ , 21 °C):  $\delta$  = 165.46, 134.59–130.54, 129.55, 127.60, 66.40, 59.03 ppm;  $^{31}\text{P}$  NMR (81 MHz,  $\text{CD}_2\text{Cl}_2$ , 21 °C):  $\delta$  = 37.2 ppm (d,  $^1J(^{103}\text{Rh}, ^{31}\text{P}) = 162$  Hz); IR (KBr):  $\tilde{\nu}$  = 3422 w, 2927 vw, 2850 vw, 1965 s, 1708 vs (C=O ester), 1626 m, 1572 w, 1435 m, 1275 m, 1145 vw, 1117 vw, 1059 vw, 747 w, 694 m cm<sup>–1</sup>; ESI-MS:  $m/z$ : 805 [ $M^+$ ]; elemental analysis (%) calcd for  $\text{C}_{41}\text{H}_{32}\text{Cl}_1\text{O}_5\text{P}_2\text{Rh}_1$  (805.1): C 61.2, H 4.0; found: C 60.9, H 4.2.

**9:** A solution of  $[\{\text{Rh}(\text{CO})_2\text{Cl}\}_2]$  (50 mg, 0.13 mmol) and **5** (178 mg, 0.26 mmol) in acetonitrile (20 mL) was stirred at room temperature for 2 h. The solution was filtered then evaporated to dryness. The resulting yellow solid was washed with diethyl ether (3 × 10 mL) and dried in vacuo (84 mg, 0.10 mmol, 77%). Crystals suitable for X-ray diffraction analysis were

grown by slow evaporation of a 1:3 acetone/hexane solution.  $^1\text{H}$  NMR (200 MHz,  $\text{CDCl}_3$ , 21 °C):  $\delta$  = 8.13–7.05 (m, 56H; ArH), 4.25–4.04 (br, 8H;  $-\text{OCH}_2-$ ), 3.58–3.22 ppm (br, 8H;  $-\text{OCH}_2-$ );  $^{13}\text{C}$  NMR (50 MHz,  $\text{CDCl}_3$ , 21 °C):  $\delta$  = 207.79, 167.93, 136.40–128.36, 69.03–68.53, 66.25–65.32 ppm;  $^{31}\text{P}$  NMR (81 MHz,  $\text{CDCl}_3$ , 21 °C):  $\delta$  = 31.96 ppm (d,  $1/J(^{103}\text{Rh}, ^{31}\text{P})$  = 161 Hz); IR (KBr):  $\tilde{\nu}$  = 3423 m, 2924 w, 2875 w, 1968 vs, 1716 vs (C=O ester), 1480 vw, 1435 m, 1275 s, 1112 m, 1063 m, 748 s, 696 s  $\text{cm}^{-1}$ ; ESI-MS:  $m/z$ : 1698 [ $M^+$ ]; elemental analysis calcd (%) for  $\text{C}_{86}\text{H}_{72}\text{O}_{12}\text{P}_4\text{Rh}_2\text{Cl}_2$  (1698.1): C 60.8, H 4.3; found: C 60.9, H 4.2.

**10:** A solution of  $[\text{Ir}(\text{cod})\text{Cl}]_2$  (50 mg, 0.07 mmol) in dichloromethane (10 mL) was added to a solution of **1** (192 mg, 0.30 mmol) in the same solvent (10 mL). After refluxing for 12 h, the resulting orange solution was filtered, and the solvent evaporated to dryness. The remaining yellow-orange solid was washed three times with diethyl ether and dried in vacuo (178 mg, 0.17 mmol, 60%).  $^1\text{H}$  NMR (200 MHz,  $\text{CDCl}_3$ , 21 °C):  $\delta$  = 8.02 (brs, 1H;  $-\text{NH}$ ), 8.06–7.02 (m, 40H; ArH), 4.98–4.13 (br, 2H;  $-\text{CH}=\text{CH}(\text{cod})$ ), 3.66–3.32 (m, 4H;  $-\text{OCH}_2-$  and  $-\text{NCH}_2-$ ), 2.39–1.73 ppm (m, 8H;  $-\text{CH}_2(\text{cod})$ );  $^{13}\text{C}$  NMR (50 MHz,  $\text{CDCl}_3$ , 21 °C):  $\delta$  = 179.11, 176.57, 166.45, 163.67, 160.61, 154.85, 154.37, 139.88–124.58, 55.11, 50.64, 49.96, 49.55, 34.37, 32.25, 31.23, 30.11, 29.77, 28.43, 26.73 ppm;  $^{31}\text{P}$  NMR (81 MHz,  $\text{CDCl}_3$ , 21 °C):  $\delta$  = 20.93 ppm (brs); IR (KBr):  $\tilde{\nu}$  = 3438 br, 3253 m, 3053 vw, 2928 s, 2854 m, 1695 vs (C=O ester), 1630 vs (C=O amide), 1533 m, 1451 vw, 1434 vw, 1367 w, 1346 vw, 1093 w, 747 w, 697 m  $\text{cm}^{-1}$ ; elemental analysis calcd (%) for  $\text{C}_{48}\text{H}_{45}\text{Cl}_1\text{Ir}_1\text{N}_1\text{O}_3\text{P}_2$  (973.5): C 59.2, H 4.7; found: C 59.5, H 4.3.

**11:** A solution of  $[\text{Ir}(\text{cod})\text{Cl}]_2$  (50 mg, 0.07 mmol) in toluene (10 mL) was added dropwise to a solution of **2** (214 mg, 0.30 mmol) in the same solvent (10 mL). After refluxing for 12 h, the resulting orange solution was filtered, and the solvent evaporated to dryness. The remaining yellow-orange solid was washed three times with diethyl ether and dried in vacuo (96 mg, 0.09 mmol, 65%).  $^1\text{H}$  NMR (200 MHz,  $\text{CDCl}_3$ , 21 °C):  $\delta$  = 8.01–6.89 (m, 33H; ArH), 4.80 (br, 2H;  $-\text{CH}=\text{CH}(\text{cod})$ ), 4.25 (br, 2H;  $-\text{OCH}_2-$ ), 3.49 (br, 2H;  $-\text{NCH}_2-$ ), 3.35 (m, 2H;  $-\text{CH}=\text{CH}(\text{cod})$ ), 2.20–1.80 ppm (m, 8H;  $-\text{CH}_2(\text{cod})$ );  $^{13}\text{C}$  NMR (50 MHz,  $\text{CDCl}_3$ , 21 °C):  $\delta$  = 170.21, 167.32, 136.53–128.64, 68.30, 60.24, 33.46, 32.17, 29.94, 29.63, 22.95 ppm;  $^{31}\text{P}$  NMR (81 MHz,  $\text{CDCl}_3$ , 21 °C):  $\delta$  = 21.64 ppm (brs); IR (KBr):  $\tilde{\nu}$  = 3427 vw, 2928 m, 2851 w, 1717 s (C=O ester), 1651 s (C=O amide), 1583 w, 1234 m, 1272 s, 1142 m, 1056 m, 746 s  $\text{cm}^{-1}$ ; ESI-MS:  $m/z$ : 1049 [ $M^+$ ]; elemental analysis calcd (%) for  $\text{C}_{54}\text{H}_{49}\text{O}_3\text{P}_4\text{Ir}_1\text{Cl}_1\text{N}_1$  (1049.6): C 61.8, H 4.7; found: C 61.9, H 4.3.

**12:** A solution of  $[\text{Ir}(\text{cod})\text{Cl}]_2$  (50 mg, 0.07 mmol) in toluene (10 mL) was added dropwise to a solution of **3** (192 mg, 0.30 mmol) in the same solvent (10 mL). After refluxing for 12 h, the resulting orange solution was filtered, and the solvent evaporated to dryness. The remaining yellow-orange solid was washed three times with diethyl ether and dried in vacuo (96 mg, 0.10 mmol, 71%).  $^1\text{H}$  NMR (200 MHz,  $\text{CDCl}_3$ , 21 °C):  $\delta$  = 8.20–6.89 (m, 28H; ArH), 4.90 (br, 2H;  $-\text{CH}=\text{CH}(\text{cod})$ ), 4.44–4.40 (br, 2H;  $-\text{OCH}_2-$ ), 4.09 (br, 2H;  $-\text{OCH}_2-$ ), 3.49 (m, 2H;  $-\text{CH}=\text{CH}(\text{cod})$ ), 2.20 ppm (m, 8H;  $-\text{CH}_2(\text{cod})$ );  $^{13}\text{C}$  NMR (50 MHz,  $\text{CDCl}_3$ , 21 °C):  $\delta$  = 167.64, 135.43–128.34, 68.30, 60.24, 33.46, 32.17, 29.94, 29.63, 22.95 ppm;  $^{31}\text{P}$  NMR (81 MHz,  $\text{CDCl}_3$ , 21 °C):  $\delta$  = 20.43 ppm (brs); IR (KBr):  $\tilde{\nu}$  = 3427 br, 2928 m, 2851 w, 1710 s (C=O ester), 1626 m, 1583 w, 1234 m, 1272 s, 1142 m, 1056 m, 746 s  $\text{cm}^{-1}$ ; ESI-MS:  $m/z$ : 1059 [ $M^+ + \text{CH}_2\text{Cl}_2$ ]; elemental analysis calcd (%) for  $\text{C}_{48}\text{H}_{44}\text{Cl}_1\text{Ir}_1\text{O}_4\text{P}_2$  (974.5): C 59.2, H 4.5; found: C 59.3, H 4.7.

**13:** An orange solution of **10** (100 mg, 0.10 mmol) in dichloromethane (50 mL) was stirred at room temperature under CO. After 5 min the resulting yellow solution was filtered, and the solvent evaporated to dryness. The remaining yellow solid was washed three times with diethyl ether/pentane (5:1, 10 mL), three times with pentane (10 mL) and dried in vacuo (45 mg, 0.05 mmol, 50%).  $^1\text{H}$  NMR (200 MHz,  $\text{CDCl}_3$ , 21 °C):  $\delta$  = 8.05 (brs, 1H;  $-\text{NH}$ ), 8.10–7.05 (m, 40H; ArH), 3.68–3.30 ppm (m, 4H;  $-\text{OCH}_2-$  and  $-\text{NCH}_2-$ );  $^{13}\text{C}$  NMR (50 MHz,  $\text{CDCl}_3$ , 21 °C):  $\delta$  = 180.13, 176.57, 166.45, 163.67, 160.61, 154.85, 154.37, 139.88–124.58, 55.11, 50.64 ppm;  $^{31}\text{P}$  NMR (81 MHz,  $\text{CDCl}_3$ , 21 °C):  $\delta$  = 27.10 ppm (brs); IR (KBr):  $\tilde{\nu}$  = 3283 m, 3053 vw, 2925 vw, 1950 vs, 1695 vs (C=O ester), 1645 s (C=O amide), 1295 m, 1275 s, 1112 m, 749 w, 744 s, 694 s  $\text{cm}^{-1}$ ; elemental analysis calcd (%) for  $\text{C}_{43}\text{H}_{36}\text{Cl}_1\text{Ir}_1\text{O}_6\text{P}_2$  (893.3): C 55.1, H 3.7; found: C 54.8, H 4.0.

**14:** An orange solution of **11** (100 mg, 0.10 mmol) in dichloromethane (50 mL) was stirred at room temperature under CO. After 5 min the

resulting yellow solution was filtered, and the solvent evaporated to dryness. The remaining yellow solid was washed three times with diethyl ether/pentane (5:1, 10 mL), three times with pentane (10 mL) and dried in vacuo (40 mg, 0.041 mmol, 41%).  $^1\text{H}$  NMR (200 MHz,  $\text{CDCl}_3$ , 21 °C):  $\delta$  = 8.01–6.89 (m, 33H; ArH), 4.25 (br, 2H;  $-\text{OCH}_2-$ ), 3.49 ppm (br, 2H;  $-\text{NCH}_2-$ );  $^{13}\text{C}$  NMR (50 MHz,  $\text{CDCl}_3$ , 21 °C):  $\delta$  = 170.21, 167.32, 136.53–128.64, 68.30, 60.24 ppm;  $^{31}\text{P}$  NMR (81 MHz,  $\text{CDCl}_3$ , 21 °C):  $\delta$  = 27.93 ppm (brs); IR (KBr):  $\tilde{\nu}$  = 3422 vw, 3053 vw, 2925 vw, 1951 vs, 1718 vs (C=O ester), 1650 s (C=O amide), 1295 m, 1275 s, 1112 m, 749 w, 744 s, 694 s  $\text{cm}^{-1}$ ; elemental analysis calcd (%) for  $\text{C}_{43}\text{H}_{36}\text{Cl}_1\text{Ir}_1\text{O}_6\text{P}_2$  (969.4): C 58.2, H 3.8; found: C 58.0, H 4.1.

**15:** An orange solution of **12** (100 mg, 0.10 mmol) in dichloromethane (50 mL) was stirred at room temperature under CO. After 5 min the resulting yellow solution was filtered, and the solvent evaporated to dryness. The remaining yellow solid was washed three times with diethyl ether/pentane (5:1, 10 mL), three times with pentane (10 mL) and dried in vacuo (45 mg, 0.05 mmol, 50%).  $^1\text{H}$  NMR (200 MHz,  $\text{CDCl}_3$ , 21 °C):  $\delta$  = 8.22–6.90 (m, 28H; ArH), 4.40–4.29 (m, 2H;  $-\text{OCH}_2-$ ), 3.74–3.71 ppm (m, 2H;  $-\text{OCH}_2-$ );  $^{13}\text{C}$  NMR (50 MHz,  $\text{CDCl}_3$ , 21 °C):  $\delta$  = 167.64, 135.43–128.34, 68.30, 60.24 ppm;  $^{31}\text{P}$  NMR (81 MHz,  $\text{CDCl}_3$ , 21 °C):  $\delta$  = 27.52 ppm (brs); IR (KBr):  $\tilde{\nu}$  = 3422 vw, 3053 vw, 2925 vw, 1944 vs, 1720 vs (C=O ester), 1434 s, 1295 m, 1275 s, 1112 m, 749 w, 744 s, 694 s  $\text{cm}^{-1}$ ; ESI-MS:  $m/z$ : 894 [ $M^+$ ]; elemental analysis calcd (%) for  $\text{C}_{43}\text{H}_{36}\text{Cl}_1\text{Ir}_1\text{O}_6\text{P}_2$  (894.3): C 55.0, H 3.6; found: C 54.6, H 4.2.

**16:** A solution of  $[\text{Ir}(\text{cod})\text{Cl}]_2$  (50 mg, 0.07 mmol) in dichloromethane (10 mL) was added dropwise to a solution of **4** (52 mg, 0.15 mmol) in the same solvent (10 mL). Then the solution was heated under reflux for 12 h. After filtration of the cooled solution, the solvent was evaporated to dryness. The remaining yellow-orange solid was washed three times with diethyl ether and dried in vacuo (96 mg, 0.10 mmol, 71%). Crystals suitable for X-ray diffraction analysis were grown by slow evaporation of a 1:3 acetone/hexane solution.  $^1\text{H}$  NMR (200 MHz,  $\text{CDCl}_3$ , 21 °C):  $\delta$  = 8.15–6.80 (m, 14H; ArH), 4.91 (m, 2H;  $-\text{CH}=\text{CH}(\text{cod})$ ), 4.42 (m, 2H;  $-\text{CH}=\text{CH}(\text{cod})$ ), 4.10–4.06 (m, 2H;  $-(\text{CO})\text{OCH}_2-$ ), 3.68–3.66 (m, 2H;  $-\text{OCH}_2-$ ), 2.42–2.20 ppm (m, 8H;  $-\text{CH}_2(\text{cod})$ );  $^{13}\text{C}$  NMR (50 MHz,  $\text{CDCl}_3$ , 21 °C):  $\delta$  = 166.80, 154.19, 140.91, 138.30, 135.22–128.67, 63.21, 50.21 ppm;  $^{31}\text{P}$  NMR (81 MHz,  $\text{CDCl}_3$ , 21 °C):  $\delta$  = 20.28 ppm (brs); IR (KBr):  $\tilde{\nu}$  = 3340 br, 2932 w, 1705 vs (C=O ester), 1627 w, 1437 vw, 1368 vw, 1274 vs, 1144 m, 1095 m, 105 ws, 747 m, 694 s  $\text{cm}^{-1}$ ; elemental analysis calcd (%) for  $\text{C}_{29}\text{H}_{31}\text{Cl}_1\text{Ir}_1\text{O}_3\text{P}_1$  (686.2): C 50.8, H 4.5; found: C 50.9, H 4.2.

**17:** An orange solution of **16** (100 mg, 0.15 mmol) in dichloromethane (50 mL) was stirred at room temperature under CO. After 5 min the resulting yellow solution was filtered, and then the solvent evaporated to dryness. The remaining yellow solid was washed three times with diethyl ether/pentane (5:1, 10 mL), three times with pentane (10 mL) and dried in vacuo (57 mg, 0.09 mmol, 60%).  $^1\text{H}$  NMR (200 MHz,  $\text{CDCl}_3$ , 21 °C):  $\delta$  = 8.22–6.90 (m, 28H; ArH), 4.40–4.29 (m, 2H;  $-\text{OCH}_2-$ ), 3.74–3.71 ppm (m, 2H;  $-\text{OCH}_2-$ );  $^{13}\text{C}$  NMR (50 MHz,  $\text{CDCl}_3$ , 21 °C):  $\delta$  = 167.64, 135.43–128.34, 68.30, 60.24 ppm;  $^{31}\text{P}$  NMR (81 MHz,  $\text{CDCl}_3$ , 21 °C): 27.52 (brs); IR (KBr):  $\tilde{\nu}$  = 3440 vw, 3054 vw, 2067.2 s, 1985 vs, 1707 s (C=O ester), 1647 m, 1579 w, 1435 s, 1277 s, 746 s  $\text{cm}^{-1}$ ; elemental analysis calcd (%) for  $\text{C}_{25}\text{H}_{19}\text{Cl}_1\text{Ir}_1\text{O}_3\text{P}_1$  (634.0): C 43.6, H 3.0; found: C 44.0, H 3.2.

**18:** A solution of  $[\text{Pt}(\text{cod})\text{I}_2]$  (50 mg, 0.09 mmol) and **2** (70 mg, 0.10 mmol) in dichloromethane (20 mL) was stirred at room temperature for 12 h. The solvent was then removed under reduced pressure. The resulting yellow solid was washed with hexane (10 mL) and dried in vacuo (70 mg, 0.06 mmol, 67%). Crystals suitable for X-ray diffraction analysis were grown by slow evaporation of a 1:3 dichloromethane/hexane solution.  $^1\text{H}$  NMR (200 MHz,  $\text{CDCl}_3$ , 21 °C):  $\delta$  = 8.03–6.25 (m, 33H; ArH), 4.73–4.71 (br, 2H;  $-\text{OCH}_2-$ ), 4.24–3.51 ppm (br, 2H;  $-\text{NCH}_2-$ );  $^{13}\text{C}$  NMR (50 MHz,  $\text{CDCl}_3$ , 21 °C):  $\delta$  = 170.42, 166.54, 144.31–140.45, 138.40–137.66, 134.85–127.97, 63.04, 48.59 ppm;  $^{31}\text{P}$  NMR (81 MHz,  $\text{CDCl}_3$ , 21 °C):  $\delta$  = 11.92 ppm ( $1/J(^{195}\text{Pt}, ^{31}\text{P})$  = 2702 Hz); IR (KBr):  $\tilde{\nu}$  = 3432 vw, 3054 m, 2922 s, 2848 m, 1707 s (C=O ester), 1619 s (C=O amide), 1593 m, 1493 m, 1480 m, 1435 s, 1252 m, 1091 m, 745 m, 694 vs, 520 vs  $\text{cm}^{-1}$ ; ESI-MS:  $m/z$ : 849 [ $M^+$ ]; elemental analysis calcd (%) for  $\text{C}_{46}\text{H}_{37}\text{NO}_3\text{P}_2\text{Pt}$  (1162.6): C 47.5, H 3.2; found: C 47.7, H 3.3.

**Catalytic runs:** In a typical experiment,  $[\text{Rh}(\text{CO})_2\text{Cl}]_2$  or  $[\text{Ir}(\text{cod})\text{Cl}]_2$  (24 mg, 0.06 mmol) and the ligand (0.12 mmol) were dissolved in methanol (4.46 mL). This solution was placed in a 100 mL stainless steel autoclave,

Table 2. Summary of X-ray single-crystal data and structure refinement parameters for the compounds **9**, **16**, **18**, **19a**, and **19b**.

	<b>9</b>	<b>16</b>	<b>18</b>	<b>19a</b>	<b>19b</b>
empirical formula	C <sub>92</sub> H <sub>84</sub> Cl <sub>2</sub> O <sub>14</sub> P <sub>4</sub> Rh <sub>2</sub>	C <sub>29</sub> H <sub>31</sub> Cl <sub>1</sub> Ir <sub>1</sub> O <sub>3</sub> P <sub>1</sub>	C <sub>46</sub> H <sub>37</sub> I <sub>2</sub> N <sub>1</sub> O <sub>3</sub> P <sub>2</sub> Pt <sub>1</sub> · CH <sub>2</sub> Cl <sub>2</sub>	C <sub>50</sub> H <sub>43</sub> I <sub>4</sub> N <sub>1</sub> O <sub>3</sub> P <sub>2</sub> Rh <sub>2</sub> · 3CH <sub>3</sub> COCH <sub>3</sub>	C <sub>50</sub> H <sub>43</sub> I <sub>4</sub> N <sub>1</sub> O <sub>3</sub> P <sub>2</sub> Rh <sub>2</sub>
crystal color	yellow	yellow	orange	red	red
molecular mass	1814.2	686.16	1247.52	1687.45	1513.21
temperature [K]	153(2)	153(2)	153(2)	153(2)	153(2)
crystal system	triclinic	monoclinic	triclinic	triclinic	triclinic
space group	<i>P</i> $\bar{1}$	<i>P</i> 2 <sub>1</sub> / <i>n</i>	<i>P</i> $\bar{1}$	<i>P</i> $\bar{1}$	<i>P</i> $\bar{1}$
<i>a</i> [Å]	10.910(5)	10.2660(9)	11.8425(12)	12.5407(12)	13.436(5)
<i>b</i> [Å]	13.533(5)	19.4528(17)	11.9247(11)	14.7810(14)	14.749(5)
<i>c</i> [Å]	14.576(5)	13.2522(12)	18.5076(18)	17.6206(17)	18.551(5)
$\alpha$ [°]	89.327(5)	90	93.712(12)	105.625(11)	105.924(5)
$\beta$ [°]	87.031(5)	105.411(10)	102.166(12)	98.237(11)	98.502(5)
$\gamma$ [°]	78.907(5)	90	117.611(11)	99.102(11)	107.114(5)
volume [Å <sup>3</sup> ]	2109.0(14)	2551.3(4)	2223.8(4)	3046.0(5)	3272.4(19)
<i>Z</i>	2	4	2	2	2
$\rho_{\text{calc}}$ [g cm <sup>-3</sup> ]	1.428	1.786	1.863	1.840	1.536
$\lambda$ [Å]	0.71073(MoK $\alpha$ )	0.71073(MoK $\alpha$ )	0.71073(MoK $\alpha$ )	0.71073(MoK $\alpha$ )	0.71073(MoK $\alpha$ )
$\mu$ [mm <sup>-1</sup> ]	0.595	5.431	4.777	2.673	2.475
<i>F</i> (000)	932	1352	1200	1636	1444
$\theta$ range [°]	0.931–25.87	1.91–25.92	1.96–25.98	1.98–25.98	2.10–25.88
unique reflections with <i>I</i> > 2 $\sigma$ ( <i>I</i> )	7621	4766	8067	11121	11768
final <i>R</i> 1, <i>wR</i> 2 <sup>[a]</sup> (observed data)	0.0327, 0.0430	0.0682, 0.0737	0.0241, 0.0536	0.0749, 0.1382	0.0567, 0.1732
parameters/restraints	516/0	314/0	551/0	358/0	504/0
GoF	0.881	0.970	0.910	0.659	0.958
residual density (max/min) [e Å <sup>-3</sup> ]	0.985/–0.817 105.411(10)	1.443/–0.806	0.907/–0.968	1.495/–1.849	6.619/–1.322

[a]  $R1 = [\sum(|F_o| - |F_c|)/\sum|F_o|]$ ;  $wR2 = \{[\sum(\omega(F_o^2 - F_c^2)^2)/\sum(\omega F_o^4)]^{1/2}\}$ .

and iodomethane (11 mmol) and water (200 mmol) were added. After purging three times with CO, the autoclave was pressurized with carbon monoxide (25 bar) and heated to 170 °C under vigorous stirring of the reaction mixture (900 rpm). After 20 min, the autoclave was cooled to room temperature, and the pressure released. The solution was filtered and analyzed by GC.

Gas chromatography was performed on a Dani86.10 gas chromatograph equipped with a split-mode capillary injection system and flame ionization detector using a Cp-wax 52-CB capillary column (25 m × 0.32 mm).

**Crystal structure determinations:** Intensity data were collected at 153 K on a Stoe Image Plate Diffraction system<sup>[31]</sup> using MoK $\alpha$  graphite-monochromated radiation. The structure was solved by direct methods using the program SHELXS-97.<sup>[32]</sup> The refinement and all further calculations were carried out using SHELXL-97.<sup>[33]</sup> Hydrogen atoms were included in calculated positions and treated as riding atoms using SHELXL default parameters. The non-hydrogen atoms were refined anisotropically, using weighted full-matrix least-squares on *F*<sup>2</sup>. Structure calculations, checking for higher symmetry and preparation of molecular plots were performed with the PLATON<sup>[34]</sup> package. Further experimental details are given in Table 2.

CCDC-178634 (**9**), CCDC-178812 (**16**), CCDC-178813 (**18**), CCDC-178933 (**19a**), and CCDC-178932 (**19b**) contain the supplementary crystallographic data for this paper. These data can be obtained free of charge via [www.ccdc.cam.ac.uk/conts/retrieving.html](http://www.ccdc.cam.ac.uk/conts/retrieving.html) (or from the Cambridge Crystallographic Data Centre, 12, Union Road, Cambridge CB21EZ, UK; fax: (+44) 1223-336-033; or deposit@ccdc.cam.ac.uk).

## Acknowledgements

This work was supported by the Fonds National Suisse de la Recherche Scientifique (grant no. 2061227.00).

- [1] K. Weissmehl, H.-J. Arpe, *Industrial Organic Chemistry*, 3rd ed., VCH, Weinheim, 1997.
- [2] G. W. Parshall, S. D. Ittel, *Homogeneous Catalysis*, 2nd ed.n, Wiley-Interscience, New York, 1992, p. 96.

- [3] F. E. Paulik, J. F. Roth, *Chem. Commun.* **1968**, 1578.
- [4] D. Forster, *J. Am. Chem. Soc.* **1976**, 98, 846–848.
- [5] D. Forster, *Adv. Organomet. Chem.* **1979**, 17, 255–267.
- [6] D. Forster, T. C. Singleton, *J. Mol. Catal.* **1982**, 17, 299.
- [7] J. F. Roth, J. H. Craddock, A. Hershman, F. E. Paulik, *Chem. Technol.* **1971**, 600–605.
- [8] A. L. Balch, B. Tulyathan, *Inorg. Chem.* **1977**, 16, 2840–2845.
- [9] T. Ghaffar, H. Adams, P. M. Maitlis, A. Haynes, G. J. Sunley, M. J. Baker, *Chem. Commun.* **1998**, 1359–1360.
- [10] J. Rankin, A. D. Poole, A. C. Benyei, D. J. Cole-Hamilton, *Chem. Commun.* **1997**, 1835–1836.
- [11] K. V. Katti, B. D. Santarsiero, A. A. Pinkerton, R. G. Cavell, *Inorg. Chem.* **1993**, 32, 5919–5925.
- [12] a) M. J. Baker, M. F. Giles, A. G. Orpen, M. J. Taylor, R. J. Watt, *J. Chem. Soc. Chem. Commun.* **1995**, 197–198; L. Gonzalvi, H. Adams, G. J. Sunley, E. Ditzel, A. Haynes, *J. Am. Chem. Soc.* **1999**, 121, 11 233.
- [13] J. Rankin, A. C. Benyei, A. D. Poole, D. J. Cole-Hamilton, *J. Chem. Soc. Dalton Trans.* **1999**, 3771–3782.
- [14] K. G. Moloy, R. W. Wegman, *Organometallics* **1989**, 8, 2883–2892.
- [15] R. W. Wegman, *Chem. Abstr.* **1986**, 105, 78526g.
- [16] J. H. Jones, *Platinum Metals Rev.* **2000**, 44, 94–105.
- [17] C.-A. Carraz, E. J. Ditzel, A. G. Orpen, D. D. Ellis, P. G. Pringle, G. J. Sunley, *Chem. Commun.* **2000**, 1277–1278.
- [18] J. E. Hoots, T. B. Rauchfuss, D. A. Wroblewski, *Inorg. Syn.* **1982**, 21, 178–179.
- [19] a) B. M. Trost, D. L. Van Vranken, *Angew. Chem.* **1992**, 104, 194–196; *Angew. Chem. Int. Ed. Engl.* **1992**, 31, 228–230; b) A. Hassner, L. Krepski, V. Alexanian, *Tetrahedron* **1978**, 34, 2069–2076; c) A. Hassner, V. Alexanian, *Tetrahedron Lett.* **1978**, 46, 4475–4478; d) E. F. V. Scriven, *Chem. Soc. Rev.* **1983**, 12, 129–161; e) C. M. Thomas, A. Neels, H. Stöckli-Evans, G. Süß-Fink, *Eur. J. Inorg. Chem.* **2001**, 12, 3005–3008.
- [20] D. Armspach, D. Matt, *Chem. Commun.* **1999**, 1073–1074.
- [21] A. J. Pryde, B. L. Shaw, B. J. Weeks, *J. Chem. Soc. Chem. Commun.* **1973**, 947–948.
- [22] W. E. Hill, D. M. A. Minahan, J. G. Taylor, C. A. McAuliffe, *J. Am. Chem. Soc.* **1982**, 104, 6001–6005.
- [23] A. J. Pryde, B. L. Shaw, B. J. Weeks, *J. Chem. Soc. Dalton Trans.* **1976**, 322–327.

- [24] A. R. Sanger, K. G. Tan, *Inorg. Chim. Acta* **1978**, *31*, L439–L440.
- [25] S. Brunie, J. Mazan, N. Langlois, H. B. Kagan, *J. Organomet. Chem.* **1976**, *114*, 225–232.
- [26] C. Bianchini, E. Farnetti, L. Glendenning, M. Graziani, G. Nardin, M. Peruzzini, E. Rocchini, F. Zanobini, *Organometallics* **1995**, *3*, 1489–1502.
- [27] a) E. K. van den Beuken, A. Meetsma, H. Kooijman, A. L. Spek, B. L. Feringa, *Inorg. Chim. Acta* **1997**, *264*, 171–183; b) H.-B. Bürgi, J. Murray-Rust, M. Camalli, F. Caruso, L. M. Venanzi, *Helv. Chim. Acta* **1989**, *72*, 1293–1302, and references therein; c) E. B. Bauer, J. Ruwwe, J. M. Martín-Alvarez, T. B. Peters, J. C. Bohling, F. A. Hampel, S. Szafert, T. Liz, J. A. Gladysz, *Chem. Commun.* **2000**, 2261–2262; d) C. G. Arena, D. Drommi, F. Faraone, C. Graiff, A. Tiripicchio, *Eur. J. Inorg. Chem.* **2001**, 247–255; e) S. K. Armstrong, R. J. Cross, L. J. Farrugia, D. A. Nichols, A. Perry, *Eur. J. Inorg. Chem.* **2002**, 141–151.
- [28] C. P. Casey, E. L. Paulsen, E. W. Beuttenmueller, B. R. Proft, B. A. Matter, D. R. Powell, *J. Am. Chem. Soc.* **1999**, *121*, 63–70, and references therein.
- [29] C.-H. Cheng, R. Eisenberg, *Inorg. Chem.* **1979**, *18*, 1418–1424.
- [30] J. V. Heras, E. Pinilla, P. Ovejero, *J. Organomet. Chem.* **1987**, *332*, 213–217.
- [31] Stoe & Cie. *IPDS Software*. Stoe & Cie GmbH, Darmstadt, Germany, **2000**.
- [32] G. M. Sheldrick, SHELXS-97 Program for Crystal Structure Determination, *Acta Crystallogr. Sect. A* **1990**, *46*, 467.
- [33] G. M. Sheldrick, SHELXL-97, Universität Göttingen, Göttingen, Germany, **1999**.
- [34] A. L. Spek, PLATON/PLUTON version Jan. 1999, *Acta Crystallogr. Sect. A* **1999**, *46*, C34.

Received: March 1, 2002 [F3916]